Transport properties in chromium-doped Ti 2 O 3 thin films

Zhenjun Wang, Jinke Tang, and Leonard Spinu

Citation: Journal of Applied Physics **97**, 10D319 (2005); doi: 10.1063/1.1852855
View online: http://dx.doi.org/10.1063/1.1852855
View Table of Contents: http://scitation.aip.org/content/aip/journal/jap/97/10?ver=pdfcov
Published by the AIP Publishing

Transport properties in chromium-doped Ti_2O_3 thin films

Zhenjun Wang and Jinke Tang[a)]
Department of Physics, University of New Orleans, New Orleans, Louisiana 70148

Leonard Spinu
Advanced Materials Research Institute, University of New Orleans, New Orleans, Louisiana 70148

(Presented on 10 November 2004; published online 6 May 2005)

In this paper, we report the transport properties of Cr-doped Ti_2O_3 thin films. The thin films were grown on α-Al_2O_3 (012) substrates by pulsed-laser deposition. X-ray diffraction and transmission electron microscopy results show that the films are single corundum phase. All of $(Cr_xTi_{1-x})_2O_3$ show semiconducting behavior. Without doping, pure Ti_2O_3 thin films show positive magnetoresistance (MR) of 23% at 2 K. The MR behavior changed dramatically after doping with Cr. Sample $(Cr_{0.1}Ti_{0.9})_2O_3$ shows MR=−360% at 2 K. All of the Cr-doped films are ferromagnetic up to room temperature. © *2005 American Institute of Physics*. [DOI: 10.1063/1.1852855]

I. INTRODUCTION

Recently, we have reported the magnetic and transport properties of Fe-, Mn-, and Cr-doped reduced-rutile Ti_nO_{2n-1}.[1–4] Following the study, we have investigated Cr-doped Ti_2O_3 thin films. The microstructure, transport and magnetic properties of Cr-doped Ti_2O_3 thin films are reported in this paper.

Ti_2O_3 has a corundum (α-Al_2O_3) structure.[5–8] Below 200 °C, Ti_2O_3 is a nonmagnetic semiconductor with an energy gap ($E_G \sim 0.1$ eV) between the top of a_{1g} band and the bottom of e_g bands of the 3*d* electrons.[9–14] The electrons in the conduction band are much heavier than the holes in the valence band, and the material exhibits positive Hall coefficient (*p* type).

Previous study reported that between Cr_2O_3 and $CrTiO_3$ the sesquioxides form a homogeneous corundum-type solid solution. In $(Cr_xTi_{1-x})_2O_3 (0.5<x<1)$ the Cr_2O_3-type antiferromagnetic (AF) structure is found with the Ti^{3+} ion acting as a simple diluent. Electron-spin resonance (ESR) gives a signal width=1600 G and $g=2.00$ for both $x=0.9$ and 1.0.[15]

II. EXPERIMENTS

$(Cr_xTi_{1-x})_2O_3$ ($x=0$, 0.04, 0.06, and 0.10) thin films were grown on α-Al_2O_3 (012) substrates by pulsed-laser deposition (PLD). Prescribed amounts of high-purity TiO_2 and Cr powders were mixed, cold pressed, and sintered to make $Cr_xTi_{1-x}O_2$ ceramic targets. The films were prepared in vacuum of 2×10^{-6} torr at substrate temperatures of 800–1000 K. The pulsed excimer laser uses KrF ($\lambda=248$ nm) and produces a laser beam with an intensity of 1–2 J/cm^2 and a repetition rate of 4 Hz. The deposition rate is between 0.3 and 0.5 Å/s, and the film thickness varies from 150 to 300 nm. The crystalline structure was investigated by x-ray diffraction (XRD) with Cu $K\alpha$ radiation and transmission electron microscopy (TEM). The magnetic properties were studied with a superconducting quantum interference device (SQUID) magnetometer. The transport properties were measured with a physical property measurement system (PPMS) from Quantum Design.

III. RESULTS AND DISCUSSION

The results of XRD and TEM show that single phase epitaxial $(Cr_xTi_{1-x})_2O_3$ films were formed by ablating the $Cr_xTi_{1-x}O_2$ targets and reduction during the deposition. Fig-

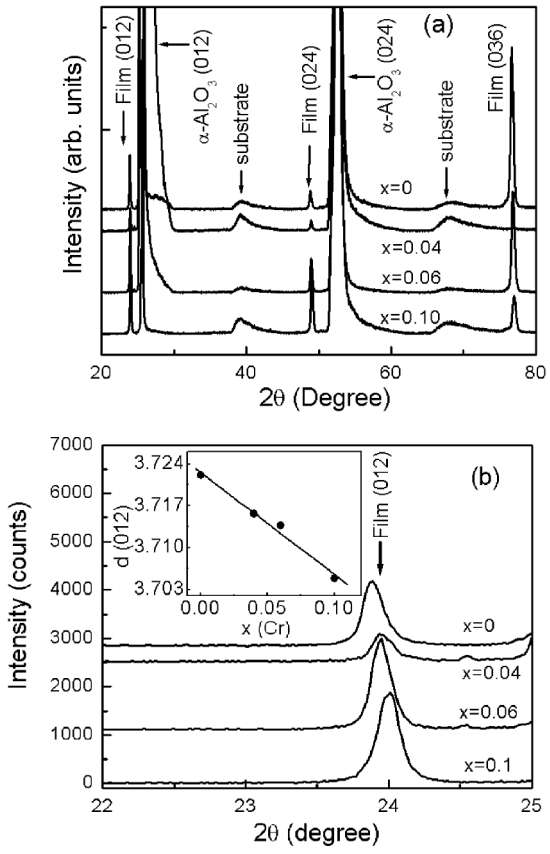

FIG. 1. (a) XRD patterns for $(Cr_xTi_{1-x})_2O_3$ ($x=0$, 0.04, 0.06, and 0.10) films. Only the reflections from the (012) family of corundum phase are observed. (b) The peak position of the (012) reflection of $(Cr_xTi_{1-x})_2O_3$ films shifts to higher angles with increasing Cr concentration *x*. Inset shows the *d* (012) values that decrease linearly with the Cr concentration.

a)Electronic mail: jtang@uno.edu

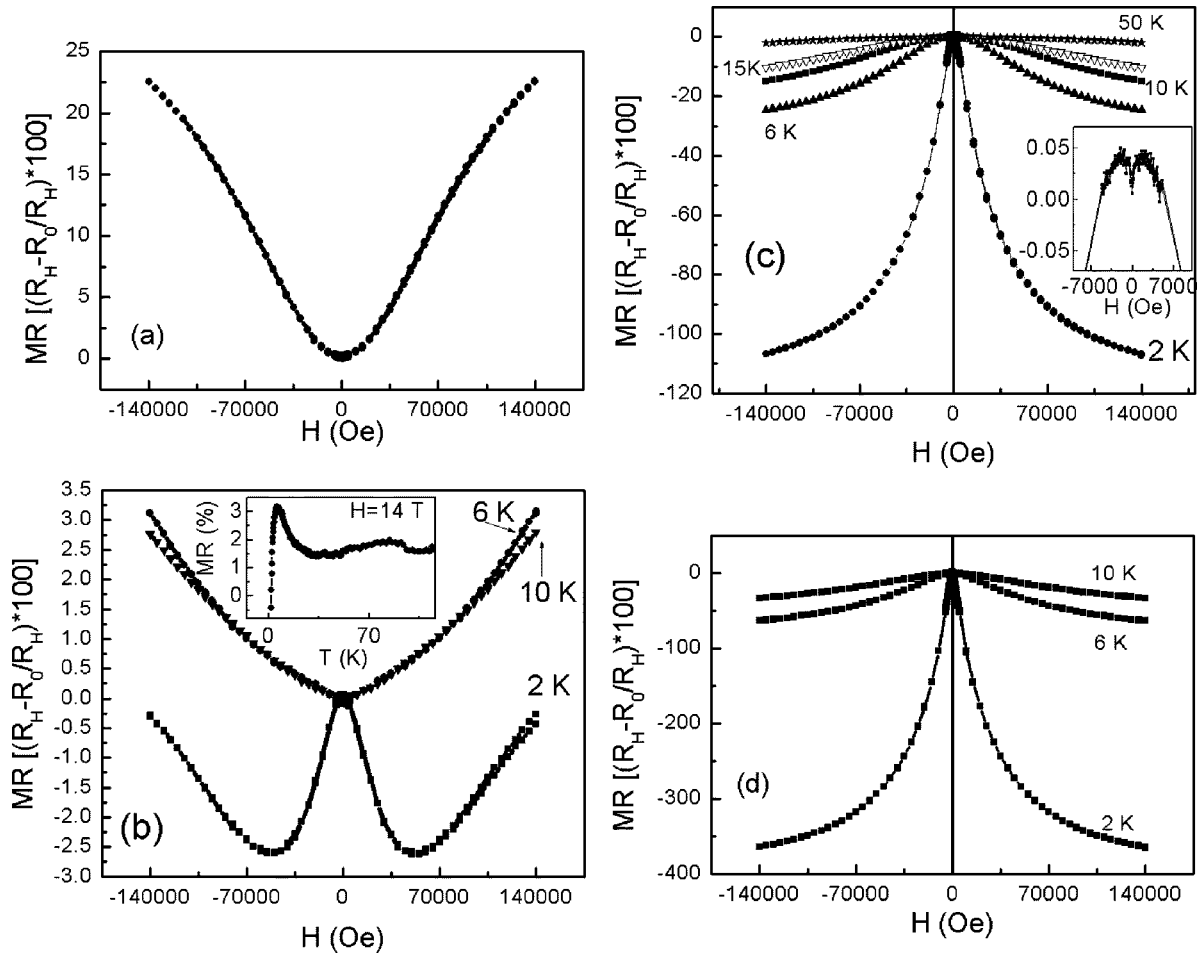

FIG. 2. MR curves for Ti_2O_3 (a), $(Cr_{0.04}Ti_{0.96})_2O_3$ (b), $(Cr_{0.06}Ti_{0.94})_2O_3$ (c), and $(Cr_{0.10}Ti_{0.90})_2O_3$ films (d). Inset of (b) shows the thermo-oscillation of magnetoresistance. Inset of (c) shows the small positive MR at 10 K for the $x=0.06$.

ure 1(a) shows the XRD patterns of $(Cr_xTi_{1-x})_2O_3$ ($x=0$, 0.04, 0.06, and 0.1) films grown on α-Al_2O_3. Only the reflections from the (012) family of corundum phase are observed. Figure 1(b) shows XRD peaks for the (012) reflection of the $(Cr_xTi_{1-x})_2O_3$ films with different Cr concentration. For $(Cr_{0.04}Ti_{0.96})_2O_3$, the (012) peak shifts to a higher angle relative to the (012) peak of Ti_2O_3, which indicates the decrease in the lattice parameters of $(Cr_xTi_{1-x})_2O_3$. This shift is further enhanced with increasing Cr content, as shown in the patterns for $(Cr_{0.06}Ti_{0.94})_2O_3$ and $(Cr_{0.10}Ti_{0.90})_2O_3$. The Cr content dependency of the *R*-axis lattice constants [*d* (012) value] is shown in the inset of Fig. 1(b). It is observed that the value of *d* (012) decreases linearly as the Cr concentration increases, which indicates that the Cr ions gradually substitute for the Ti ions in the films without changing the corundum structure.

Transport measurements with PPMS show that the films exhibit a semiconducting behavior—increasing resistivity with decreasing temperature. The carriers are *p* type for both doped and undoped films. The Hall effect of the films was measured with a four-probe method at room temperature. A carrier density of $1.2\times10^{21}\,cm^3$ was estimated for $(Cr_{0.06}Ti_{0.94})_2O_3$ from the Hall-effect measurements. All films do not exhibit anomalous Hall effect at room temperature. It is underway to measure the Hall effect at higher and lower temperatures, trying to observe the anomalous Hall effect at various temperatures.

The magnetoresistance ($MR=(R_H-R_0)/R_H\times100\%$) was measured with magnetic field perpendicular to the film plane for Ti_2O_3 and $(Cr_xTi_{1-x})_2O_3$ at various temperatures and the results are shown in Fig. 2. The MR at 2 K for Ti_2O_3 reaches +23% at 140 kOe, as Fig. 2(a) shows. This large positive MR is in agreement with previous data and is explained with a two-band model where both electrons and holes participate in the transport.[16]

Figure 2(b) shows MR for $x=0.04$ samples, at lower field, the MR is negative, while positive MR dominates in high fields at 2 K. Positive MR was observed at 6 and 10 K for $x=0.04$ films. Inset of Fig. 2(b) shows the thermo-oscillation of magnetoresistance. With 14-T constant magnetic fields, the temperature sweep caused two peaks in the magnetoresistance at about 7 and 84 K. Such peaks in the magnetoresistance were observed in $Hg_{1-x}Mn_xTe$.[17] The strong temperature dependence of the energies at which the Landau levels occur suggests that at a constant magnetic field (that provides the Landau quantization), the temperature sweep will cause the crossing of various Landau levels with the Fermi energy, if the carrier concentration in a sample is properly chosen. These crossings will then lead to successive peaks in the magnetoresistance of the sample as a function of temperature.[18]

The MR is negative and takes a giant value of −107% and −365% at 2 K in 140 kOe for $x=0.06$ and 0.10, respectively, as shown in Figs. 2(c) and 2(d). The magnitude of the

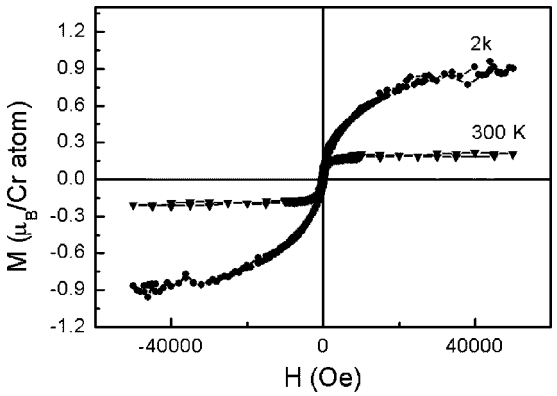

FIG. 3. Hysteresis loops of $(Cr_{0.06}Ti_{0.94})_2O_3$ film measured with a SQUID at $T=2$ and 300 K.

negative MR of $(Cr_{0.06}Ti_{0.94})_2O_3$ and $(Cr_{0.10}Ti_{0.90})_2O_3$ in high magnetic field decreases with increasing temperature. The inset of Fig. 2(c) shows the low-field region of the MR curve for $x=0.06$. At 10 K, the MR for $x=0.06$ is positive in $H<5$ kOe, reaching the maximum around 2 kOe, and turns to negative as the magnetic field goes above 5 kOe. Similar MR behavior in low fields was observed in $(Ga_{0.947}Mn_{0.053})As$ thin films and the small positive magnetoresistance disappeared when magnetic field was applied parallel to the sample plane.[19] While in our sample $x=0.06$, the small positive magnetoresistance in lower field was found in field orientations both perpendicular and parallel to the film plane.

In order to understand the magnetoresistance, we have studied the magnetic properties of the films. The results from SQUID measurements show that all of the Cr-doped films are ferromagnetic up to 400 K. Figure 3 shows magnetic hysteresis loops for $(Cr_{0.06}Ti_{0.94})_2O_3$ at 2 and 300 K. The saturation moment M_s at 2 K is 0.5, 0.91, and $0.87\mu_B$/Cr for $x=0.04$, 0.06, and 0.10, respectively. M_s initially increases with x then decreases slightly upon further increase of Cr doping. The room-temperature saturation moments are smaller, e.g., $M_s=0.2\mu_B$/Cr for $x=0.06$. Its coercivity is 50 Oe at 300 K as compared to 350 Oe at 2 K. The magnetization of $(Cr_{0.06}Ti_{0.94})_2O_3$ film at 2 K does not reach saturation at 50 kOe. The *M-H* curve consists of two components. One is a ferromagnetic part which corresponds to the lower field hysteresis loop and the other is the paramagnetic component.

To discuss the giant negative magnetoresistance for the $x=0.06$ and 0.1 film, one possible explanation is based on polaron theory. The bound magnetic polaron (BMP) is the characteristic collective state of diluted magnetic semiconductors. An exchange interaction of localized carriers with magnetic ions leads to the formation of bound magnetic polarons.[20–24] A bound polaron consists of the localized carrier and surrounding cloud of Cr spins polarized via *p-d* exchange interaction. Without magnetic field, the magnetic polarons have to move through the sea of Cr more or less randomly oriented spins. Their motion involves flipping many Cr spins, making the polarons massive and immobile. With increasing magnetic field, all Cr spins are gradually aligned to the direction of the applied magnetic field, increasing the mobility of the carriers. The negative magnetoresistance is attributed to smearing of the polaronic cloud with increasing magnetic field,[25] corresponding to the slowly increasing part of magnetization in the high-field region shown in Fig. 3.

IV. CONCLUSIONS

The experimental results show that Cr ions systematically substituted for the Ti ions in $(Cr_xTi_{1-x})_2O_3$ films. The $(Cr_{0.10}Ti_{0.9})_2O_3$ films show a negative giant magnetoresistance as large as −365% at 2 K, while the undoped film shows a positive giant magnetoresistance of +23%. The Cr-doped samples exhibit ferromagnetism up to 400 K. They are *p*-type semiconductors with a carrier density of about 1.2×10^{21} cm^3 for the $x=0.06$ sample.

ACKNOWLEDGMENTS

This work was supported by Sharp Laboratories of America and by Louisiana Board of Regents Support Fund Grant No. LEQSF(2004-07)-RD-B-12.

[1]Z. Wang, J. Tang, H. Zhang, V. Golub, L. Spinu, and L. D. Tung, J. Appl. Phys. **95**, 7381 (2004).
[2]Z. Wang, J. Tang, Y. Chen, L. Spinu, W. Zhou, and L. D. Tung, J. Appl. Phys. **95**, 7384 (2004).
[3]Z. Wang, W. Wang, J. Tang, L. D. Tung, L. Spinu, and W. Zhou, Appl. Phys. Lett. **83**, 518 (2003).
[4]Z. Wang, J. Tang, L. D. Tung, W. Zhou, and L. Spinu, J. Appl. Phys. **93**, 7870 (2003).
[5]C. E. Rice and W. R. Robinson, Acta Crystallogr., Sect. B: Struct. Crystallogr. Cryst. Chem. **33**, 1342 (1977).
[6]C. E. Rice and W. R. Robinson, Mater. Res. Bull. **11**, 1355 (1976).
[7]S. C. Abrahams, Phys. Rev. **130**, 2230 (1963).
[8]R. E. Newham and Y. M. de Haan, Z. Kristallogr. **117**, 235 (1962).
[9]J. B. Goodenough, in *Progress in Solid State Chemistry*, edited by H. Reiss (Pergamon, New York, 1971), Vol. 5, p. 280.
[10]J. M. Honig and T. B. Reed, Phys. Rev. **174**, 1020 (1968).
[11]T. C. Chi and R. J. Sladek, Phys. Rev. B **7**, 5080 (1973).
[12]H. L. Barros, G. V. Chandrashekhar, T. C. Chi, J. M. Honig, and R. J. Sladek, Phys. Rev. B **7**, 5147 (1973).
[13]S. H. Shin, G. V. Chandrashekhar, R. E. Loehman, and J. M. Honig, Phys. Rev. B **8**, 1364 (1973).
[14]G. Luckovsky, J. W. Allen, and P. Allen, Inst. Phys. Conf. Ser. **43**, 465 (1979).
[15]*Metallic Inorganic Compounds Based on Transition Elements: Perovskites II, Oxides with Corundum, Ilmenite, and Amorphous Structures*, Landolt-Börnstein, New Series, Group III, edited by Y. Endoh, K. Kakurai, and A. K. Katori (Springer Heidelberg, Berlin, 1994), Vol. 27/F3, p. 235.
[16]J. M. Honig, Rev. Mod. Phys. **40**, 748 (1968).
[17]M. Dobrowolska, W. Dobrowolski, R. R. Galazka, and J. Kossut, Solid State Commun. **30**, 25 (1979).
[18]J. K. Furdyna and J. Kossut, Semicond. Semimetals **25**, 207 (1988).
[19]F. Matsukura, H. Ohno, A. Shen, and Y. Sugawara, Phys. Rev. B **57**, R2037 (1998).
[20]P. A. Wolff, R. N. Bhatt, and A. C. Durst, J. Appl. Phys. **79**, 5196 (1996).
[21]P. A. Wolff, in *Diluted Magnetic Semiconductors*, Semiconductors and Semimetals, edited by J. K. Furdyna and J. Kossut (Academic, New York, 1988), Vol. 25, p. 413.
[22]T. Dietl and J. Spalek, Phys. Rev. Lett. **48**, 355 (1982).
[23]T. Kasuya, A. Yanase, and T. Takeda, Solid State Commun. **8**, 1543 (1970).
[24]E. L. Nagaev, Sov. Phys. JETP **29**, 545 (1969).
[25]S. von Molnar, J. Flouquet, F. Holtzberg, and G. Remenyi, Phys. Rev. Lett. **51**, 706 (1983).